Hindawi
Mathematical Problems in Engineering
Volume 2021, Article ID 1625282, 16 pages
https://doi.org/10.1155/2021/1625282

Research Article

Novel Application of the Roof-Cutting-Type Gob-Side Entry Retaining in Coal Mine

Jiong Wang[1,2], **Wenfei Li**[1,2], **Daoyong Zhu**[1,2], **Weili Gong**[1,2] and **Yi Su**[1,2]

[1]*State Key Laboratory of Geomechanics & Deep Underground Engineering, China University of Mining & Technology, Beijing 100083, China*
[2]*School of Mechanics and Civil Engineering, China University of Mining & Technology, Beijing 100083, China*

Correspondence should be addressed to Jiong Wang; wangjiong0216@163.com

Received 16 April 2021; Accepted 7 May 2021; Published 24 May 2021

Academic Editor: Gan Feng

In this study, the roof-cutting-type gob-side entry retaining is introduced, and its application in medium-thickness coal seams is studied. Based on the analysis of the construction procedure and principle, the mechanical model of the retained roadway structure and cantilever beam formed by roof cutting was established, and the support resistance and roof deformation were obtained. In addition, through technological design analysis and numerical simulation, the parameters of roof cutting were determined. The roof-cutting height and angle were designed to be 9 m and 15°, respectively. Flac3 D was used to analyze the stress evolution law under different mining conditions. The stress on the integrated coal side and roof subsidence was lower when the roof-cutting height was 8~10 m and the cutting angle was 15°. Through field monitoring, the roof pressure, gob-side lateral gangue retaining pressure, anchor cable stress, and deformation of the surrounding rock eventually reached a stable state. This indicates that the roof cutting can effectively cut down the overlying strata over the gob and form a stable entry structure to meet the requirements of the next working face.

1. Introduction

The waste of coal energy has attracted attention due to the general increase in the degree of mining mechanization [1–3]. To ensure the safety of underground work, the traditional longwall mining method balances the roof pressure in the remaining coal pillars, but the waste of coal resources is more serious [4, 5]. Therefore, the traditional gob-side entry retaining (GSER) technology has been developed to solve the problem of wasting resources, that is, use certain technical means to retain the crossheading, and serve the next working face [6], as shown in Figure 1(b). This technology realizes nonpillar mining, increases the recovery rate, reduces the development ratio, and provides advantages in ventilation and gas accumulation control [7–9]. Therefore, it is widely used.

Although the traditional GSER solves the resource waste problem [10, 11], it also has limitations: it has complex construction technology, it has high costs [9], most of the backfills are rigid materials and thus do not largely deform [12], and overwhelming under concentrated stress occurs, eventually resulting in instability of the roadway [13, 14]. At present, there are many studies on the stability of retained roadway and gob-side support body. The study of stability mainly focuses on the deformation characteristics of the retained roadway [15] and the stress distribution characteristics under the influence of mining. To understand its deformation and failure mechanism, supporting measures in roadways were performed [16]. Research on GSER mainly focuses on the material and its mechanical properties or builds the corresponding mechanical model and proposes a method to determine the main parameters of the supporting body [17–19]. Some researchers have conducted simulation experiments to study the influence of the fracture of overlying strata on the stability of the retained roadway under different geological conditions, and simulation analysis of the related roadside filling technology [20, 21]. The mentioned studies have made important contributions to the

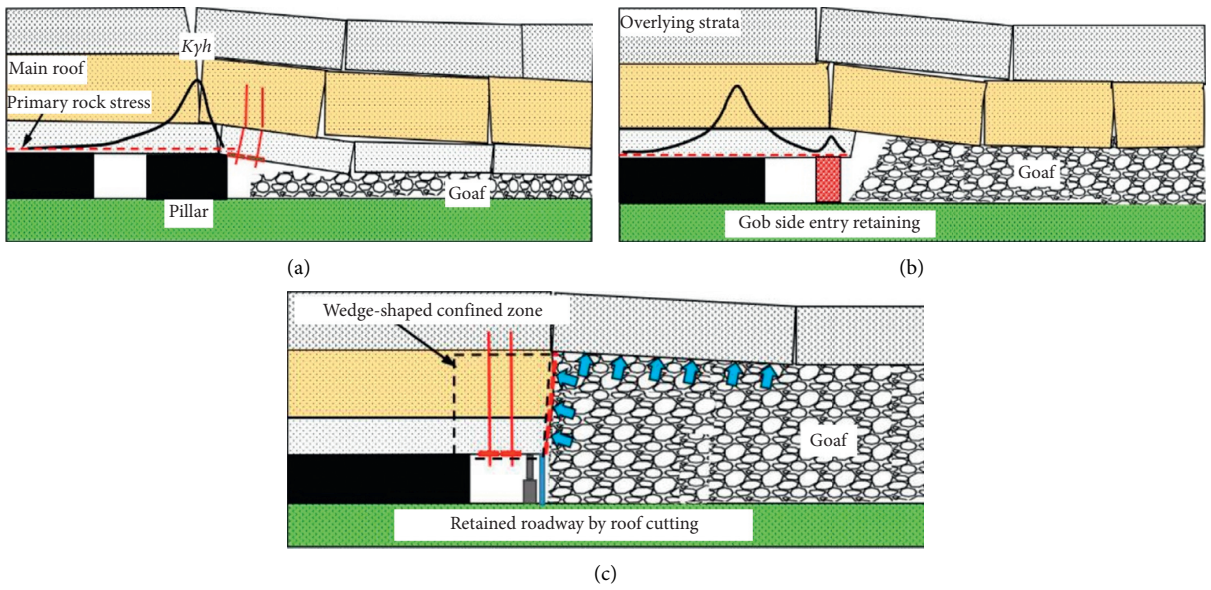

Figure 1: Principle of roadway retained. (a) Coal pillar mining. (b) Traditional GSER. (c) GSER by roof cutting.

development of GSER technology, but the essential problem remains unresolved. It mainly includes two aspects: one is the deformation of the surrounding rock caused by the rotation and subsidence of the strata above the retained roadway; the other is the fracture of the overlying hard roof into a structure of transferring stress through mutual extrusion, as shown in Figure 2(b). Therefore, the surrounding rock of the retained roadway is still under the stress environment of the traditional coal-mining mode.

To fundamentally improve the stress distribution of surrounding rock, an in-depth study was conducted based on the field application of roof-cutting-type GSER. Using theoretical analysis and numerical simulation, we analyzed the surrounding rock movement law and performed field monitoring verification. Our study contributes to a better understanding of the development of GSER technology in a medium-thick coal seam.

2. Gob-Side Entry Retaining by Roof Cutting

2.1. Construction Procedure. Figure 2 shows the main construction steps of the roof-cutting-type GSER [22, 23]. The first step: the constant resistance and large deformation (CRLD) anchor cables are adopted to strengthen the original support in the prereserved roadway area. The second step: the bidirectional energy-cavity blasting (BECB) technology is carried out along the roof beside the gob, shown in Figures 2(a) and 2(b). The third step: the gangue retaining support is carried out along the cutting-line with the advance of the working face, so as to prevent the collapsed rock from entering the reserved roadway area. Generally, the measures of retaining gangue are "single hydraulic pillar + I-shaped steel (or U-shaped steel + reinforcing mesh)." The last step: withdraw the temporary support when the support section is far away from the working face and the surrounding rock movement is stable. At this time, the retained roadway is completed, it can serve the next working face mining, and thus it realizes the mining mode of a single roadway without coal pillars.

2.2. Principle. Figure 1 shows the surrounding rock structure of the retained roadway under different retaining process conditions. As shown in Figure 1(c), the roof cutting interrupts the stress transfer path between the roof strata of the retained roadway and overlying strata above the goaf, shown in Figures 1(a) and 1(b), caused by mutual compression, and Kγh is the peak lateral support pressure. Moreover, the collapsed strata can use its bulk increase character to support the upper strata, reduce the rotary subsidence of the upper strata, and optimize the stress environment of the retained roadway [24]. Compared with traditional mining technology, this technology changes the stress environment in the area near the retained roadway and also changes the law of strata movement in the vicinity, reduces the deformation of surrounding rock, and guarantees the safe use of the retained roadway.

2.3. Key Technologies. According to the analysis of the construction procedure and principle, the roof-cutting-type GSER has two key technologies: the CRLD anchor cable reinforced support and the roof cutting by directional blasting.

2.3.1. Constant Resistance and Large Deformation Cable Support. As shown in Figure 3, the retained roadway generally experiences the influence of advanced stress, mining dynamic pressure, and reuse stage, and the surrounding rock deformation and stress of the anchor bolt continue to increase. At present, the elongation of the common anchor bolt is low, and it cannot adapt to the large deformation of the surrounding rock. The anchor bolt

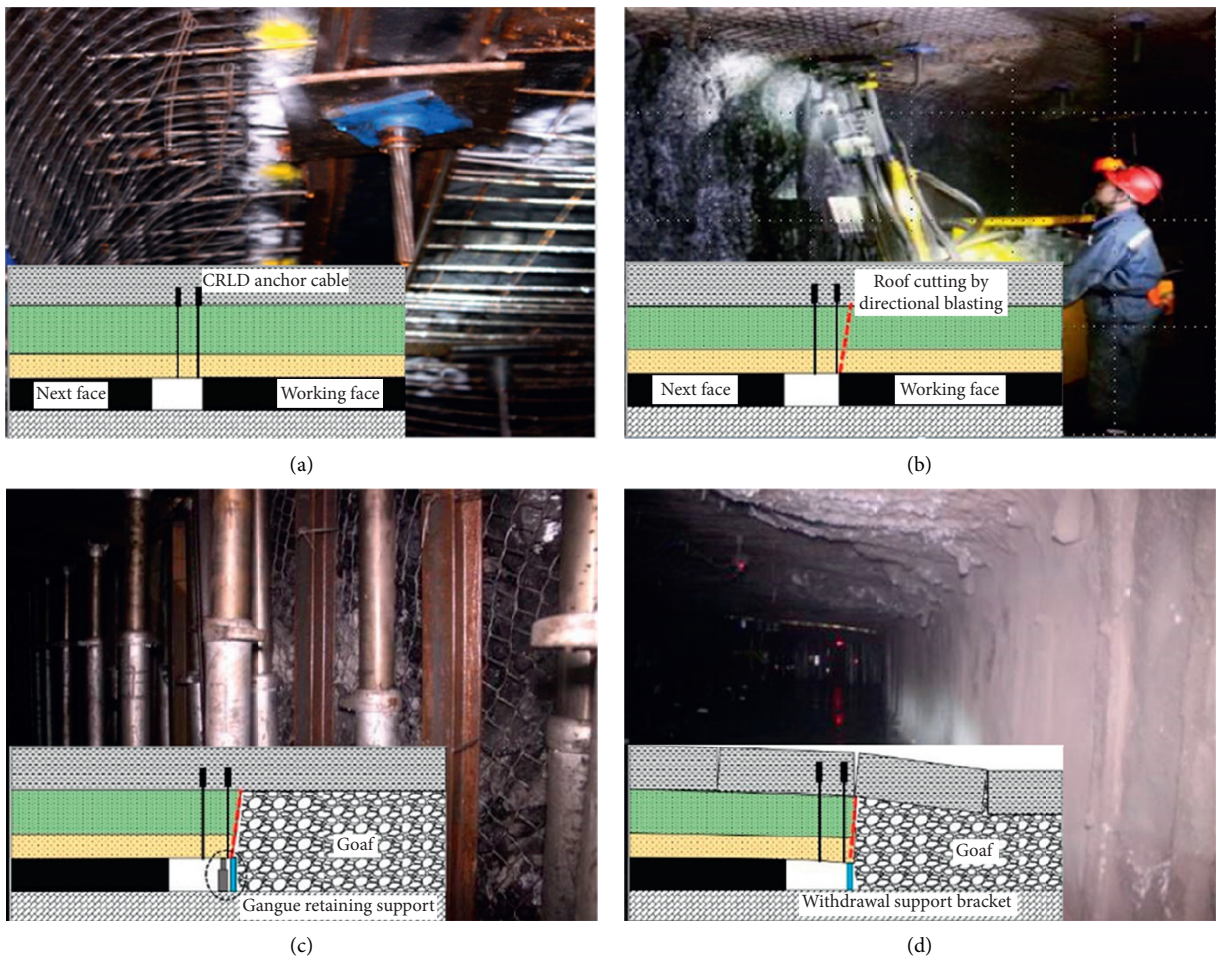

Figure 2: Process of GSER by roof cutting. (a) CRLD anchor cables reinforce support. (b) Roof cutting by directional blasting. (c) Gangue retaining support. (d) Withdraw support bracket.

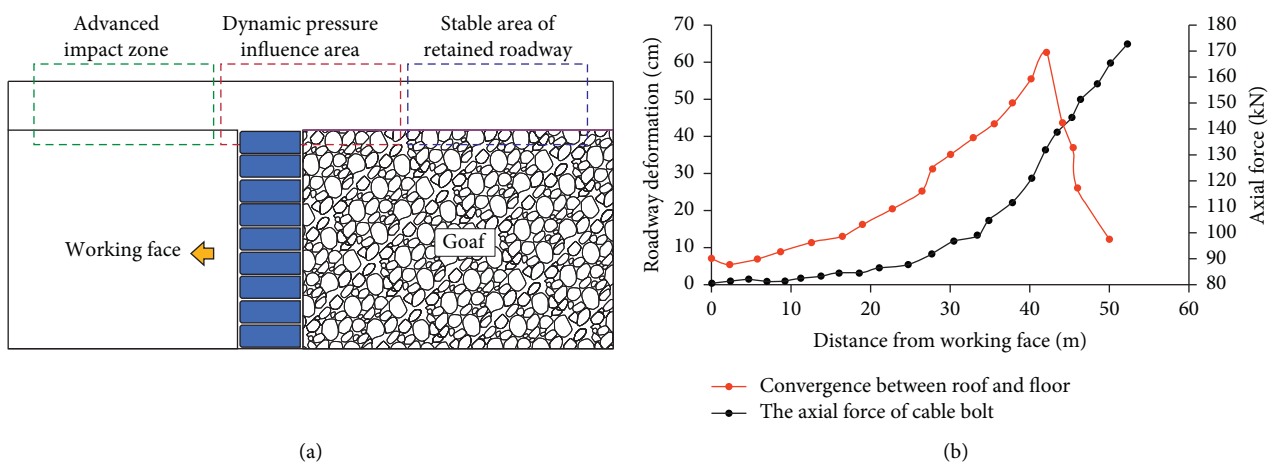

Figure 3: (a) Partition of the retained roadway. (b) Roadway deformation under traditional support.

support strength considerably decreases, its impact resistance is significantly reduced, and it is not conducive to underground safe construction. Therefore, in the process of retaining the roadway, the CRLD anchor cable is used to reinforce the original support. Figure 1(b) shows the deformation curve of the surrounding rock and the stress of the ordinary anchor bolt in the process of the traditional retaining roadway. The deformation exceeds 500 mm, and the anchor bolt breaks after the stress reaches a maximum value of 180 kN.

Figures 4(a) and 4(b) show the main structure of the anchor cable and the constitutive model and working principle, respectively [25, 26]. There are two main stages of deformation: the elastic deformation and in sequence the constant resistance tensile deformation. When the surrounding rock deformation is small, the axial force acting on the bolt is less than the constant resistance, and thus, the rod body is in the elastic state and produces elastic deformation. The deformation of the surrounding rock is resisted by the elastic deformation of the rod body. When the deformation is large and the axial force is larger than the constant resistance, the cone slides through the sleeve and generates constant resistance; i.e., the CRLD cable can produce constant support resistance under the condition of large deformation. Therefore, it is used for retained roadway support. Figure 4(b) shows the stress value of the cable at different deformation stages, which can be calculated as follows [25]:

$$P = \begin{cases} kx, & x < x_0, \\ p_{\max}, & x \geq x_0. \end{cases} \tag{1}$$

The deformation energy absorbed at different deformation stages is

$$W = \begin{cases} \dfrac{kx^2}{2}, & x < x_0, \\ \dfrac{kx^2}{2} + p_{\max}(x - x_0), & x \geq x_0. \end{cases} \tag{2}$$

2.3.2. Directional Blasting Technology. After strengthening the roadway support with the CRLD anchor cable, the next step is the roof cutting, which is also called bilateral cumulative tensile blasting technology [22]. Its main steps are to regularly drill holes along the roof and charge for blasting, cutting the overlying roof strata. However, when the conventional blasting method is employed (Figure 5(a)), the surrounding rock is damaged in large areas, and there is a serious risk of accidents, such as roof caving. Therefore, before charging, a guide pipe with two rows of guide holes should be installed in the borehole, such that the stress and energy generated by blasting can be transmitted from the guide holes to the surrounding rock surface, making the overlying strata crack along the set direction, and minimizing the damage of the rock mass, as shown in Figure 5(b).

From the above blasting analysis, it can be seen that reasonable control of the spacing of blasting holes is significantly important to maintain the stability of the surrounding rock. By studying cumulative blasting, [22] the peak stress generated can be deduced as follows:

$$\sigma_b = \sigma_h \left(\frac{r_e}{r_b}\right)^{2k} \left(\frac{L - L_0 - L_S}{L - L_S}\right)^{\gamma} \frac{2}{1 + (\rho_0/\rho_S)} \varepsilon, \tag{3}$$

where r_e is the radius of the cartridge, r_b is the hole diameter of the blast hole, σ_h is the initial detonation pressure, L is the hole depth, L_0 is the air interval length in the blast hole, L_S is the plugging length of the blast hole, ρ_0 is the explosive density, ρ_S is the rock mass density, and ε is the cumulative energy coefficient, $\varepsilon \geq 1$.

According to the attenuation law of the stress wave in the rock mass, the calculation formula for the blasting stress damage range r_1 is as follows [24]:

$$r_1 = r_b \left[\frac{\lambda \sigma_b}{(1 - D_0)\sigma_0 + p_0}\right]^{(1/a)}, \tag{4}$$

where λ is the lateral pressure coefficient, D_0 is the initial damage of the rock mass, σ_0 is the tensile strength of the rock mass, α is the attenuation index of the explosion stress wave in the rock mass, and $\alpha = 2 - \mu/1 - \mu$.

The above analysis is generally used to design the spacing of blasting holes. In addition to controlling the proper spacing, the height and angle are also important design parameters. The inclination angle is determined by the site condition and numerical simulation and is commonly less than 30°. The determination of the roof-cutting height is related to the lithology and mining height of the working face. The calculation principle is shown in Figure 6. Assuming that there are m rock layers within the roof cutting, the rock layers are marked as "1, 2, 3,. . .,m" from bottom to top. Theoretically, the caving rocks should fill the goaf below; that is, the filling height of the collapsed rock should be equal to the sum of the thicknesses of the coal seam and the rock strata within the range of roof cutting.

The following can be obtained:

$$\begin{aligned} H_1 + H_2 + \cdots H_m + M &= K_1 \cdot H_1 + + \cdots + K_m \cdot H_m, \\ K_P &= \frac{K_1 \cdot H_1 + K_2 \cdot H_2 + \cdots + K_m \cdot H_m}{\sum_{i=1}^{m} H_i}. \end{aligned} \tag{5}$$

The roof-cutting height is

$$H_Q = \sum_{i=1}^{m} H_i = \frac{M}{\left(K_p - 1\right)}, \tag{6}$$

where H_Q is the roof-cutting height; M is the thickness of the coal seam; $k_1, k_2, \ldots, k_m$ are the coefficients of broken expand of the first, second, ..., m-th layers, respectively; $H_1, H_2, \ldots, H_m$ are the rock thicknesses of the first, second, ..., m-th layers, respectively; and k_p is the average coefficient of broken expand.

2.3.3. Gangue Retaining Support. After mining, to prevent the caved rock from rushing into the retained roadway, gangue retaining support is needed. The main form of gangue retaining is usually "support bracket + retractable gangue retaining 29# U-steel + mesh reinforcement." The length of 29# U-steel is 2 m and 2.5 m, and the spacing is 500 mm. It is connected by two pairs of flanges. The upper and lower ends of the flange are 50 mm away from the lap end of the U-steel, respectively. It is not less than 300 mm below the floor. Besides, within the influence range of dynamic pressure, steel mesh is used to fix the duct cloth for

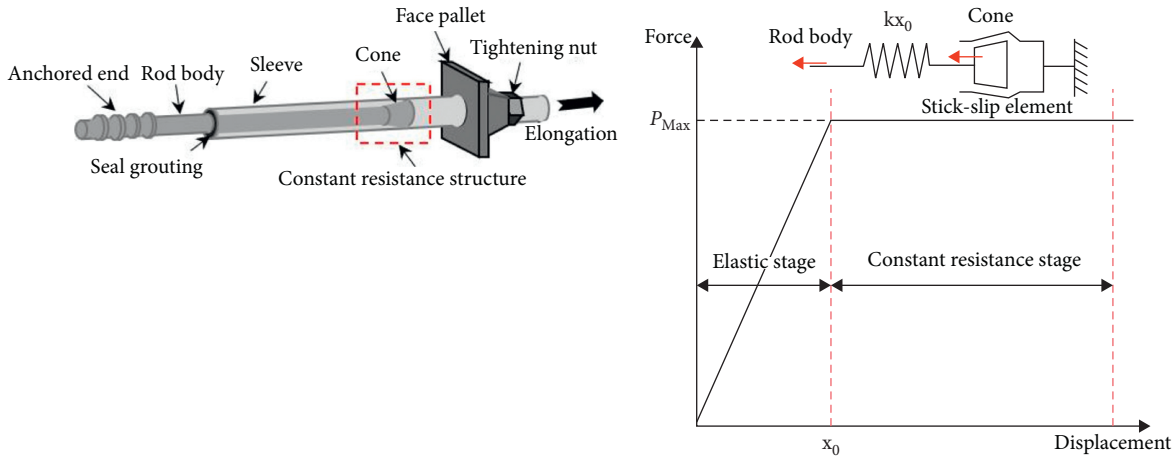

Figure 4: (a) Basic structure of CRLD anchor cable. (b) Force-displacement curve and constitutive elements.

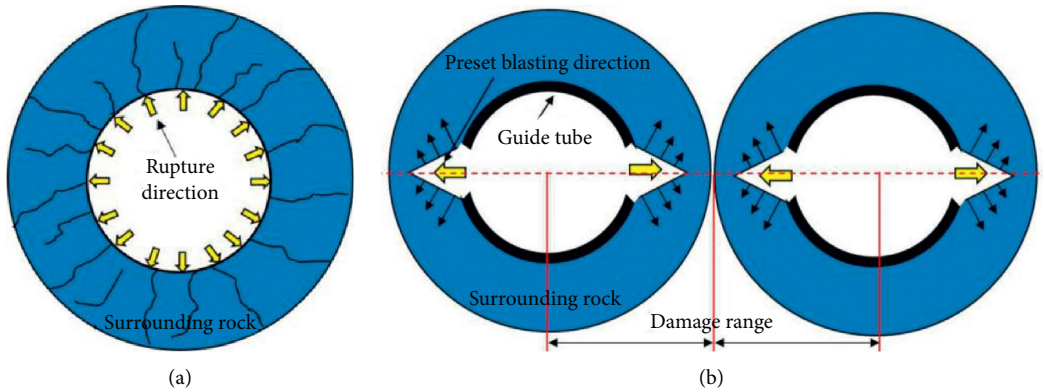

Figure 5: Comparison of drilling and blasting.

preliminary air leakage prevention, and spray treatment is used after stabilization.

2.4. Mechanical Model. Compared with the traditional filling type GSER, the surrounding rock structure fundamentally changes due to the retaining roadway process; therefore, it is necessary to study the deformation mechanism and then combine it with the field application to develop the corresponding supporting measures. As shown in Figure 1(c), owing to the roof cutting, a wedge-shaped confined zone is formed above the retained roadway. It can be regarded as a cantilever structure; therefore, the mechanical model of the retained roadway was established, as shown in Figure 7. The self-weight of the strata above the retained tunnel can be regarded as uniform load, and the support in the roadway can be regarded as uniform stress. The support of the caved rock mass in the goaf to the upper stratum can be regarded as uniform stress, and the concentrated force on the right side of the retained roadway is the support of the single pillar. It can be seen that the main parameters of the model are the support resistance of a single hydraulic prop and the deformation of the cantilever beam; thus, the solution of the model was analyzed.

The support resistance at the roof-cutting side of the reserved roadway is as follows [23]:

$$p_d = \frac{M_b + \left(N_c + qc - f_g \cdot c\right)(a+b) + (1/2)(q+q_0)(a+b)^2 - T_c \cdot \left((h/2) - \Delta S_B\right) - M_0 - \int_0^a \sigma_0 (a-x)\,\mathrm{d}x - p_s b (a + (b/2))}{a+b}. \tag{7}$$

where p_d is the support resistance of the single pillar, M_b is the ultimate bending moment of the upper strata, N_c is the shear force, f_g is the support force of the gangue in the goaf, q is the self-weight, q_0 is the self-weight of the direct roof, a is

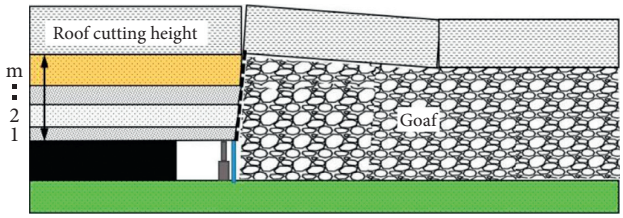

Figure 6: Schematic diagram of the roof-cutting height.

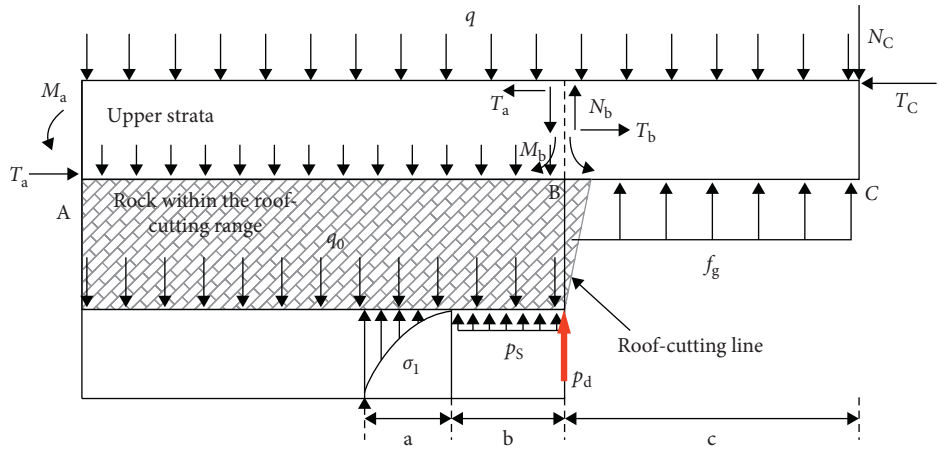

Figure 7: Surrounding rock structure after roof cutting.

the width of the limit equilibrium area, b is the roadway width, c is the length of block BC, ΔS_c is the sinking value of end C when block AC is cut off, ΔS_B is the subsidence of the B end, and h is the thickness of the old roof rock block.

The displacement of the cantilever beam can be obtained from Figure 7 as follows:

$$y = \frac{(p_r - p_s)x^2}{24EI}\left(6l^2 + x^2 - 4lx\right) - \frac{p \sin \beta x^2}{6EI}(3l - x). \tag{8}$$

Based on the above analysis of support resistance and surrounding rock deformation, the required support resistance and deformation tendency of the retained roadway can be preliminarily obtained and provide a certain reference for the support and gangue retaining support in the roadway.

3. Field Application

3.1. Engineering Background. The Dianping coal mine is located in Lvliang City, Shanxi province, as shown in Figure 8. The depth of 200 working faces is 360 m, the length of open-off cut is 220 m, the length of the crossheadings is 1088 m, the length of the open-off cut to the stop line is 942 m, the average coal seam dip angle is 4°, and the average thickness of the coal seam is 3.1 m. The designed retained roadway was used as the return air roadway. The layout of the working face is shown in Figure 8(b). Figure 8(c) shows the lithology of the roadway roof and floor. The direct floor of the working face is deep grey sandy mudstone with an average thickness of 3.3 m; the old floor is medium-grained sandstone with an average thickness of 2.8 m. From the bottom to the top of the coal seam roof, there are 2.1 m thick sandy mudstone, 6.1 m thick medium sandstone, 0.7 m thick sandy mudstone, 2.4 m thick coal interlayer, and 3.0 m thick limestone.

3.1.1. Support Design. Figure 9(a) shows the support section. The roof adopted a 20 × 2000 mm steel bolt, metal mesh, and steel bar ladder for combined support. The row and line space between the bolts was 940 × 1000 mm, with six bolts in each row. The two sides of the roadway were supported by a 16 × 1600 mm steel bolt and plastic mesh, and the row and line space between the bolts was 1200 × 1000 mm. An anchor cable with a size of Φ 18.9 × 6200 mm and channel steel was also used to strengthen the roof support, two rows of anchor cables were arranged along the roadway, and the row and line space were 2350 × 1000 mm. Based on the traditional support scheme, two rows of CRLD anchor cables were arranged: the first 500 mm away from the gob, with row spacing of 1000 mm; and the second in the middle of the roadway, with row spacing of 2000 mm. In the first row, cables were connected by a W steel belt.

The self-circulation portal hydraulic support was also used for support in the retained roadway. Furthermore, the roof broken area increased the single pillar to strengthen the support. The length of the portal hydraulic support was 2.8 m, the working resistance was 2040 kN, the designed row distance was 2000 mm, and the working resistance of the single prop was 280 kN.

Figure 9(b) shows the charge structure of the blasting hole, and the depth of the blasting hole is 8 m. Based on the cumulative blasting analysis and in situ tests, the distance

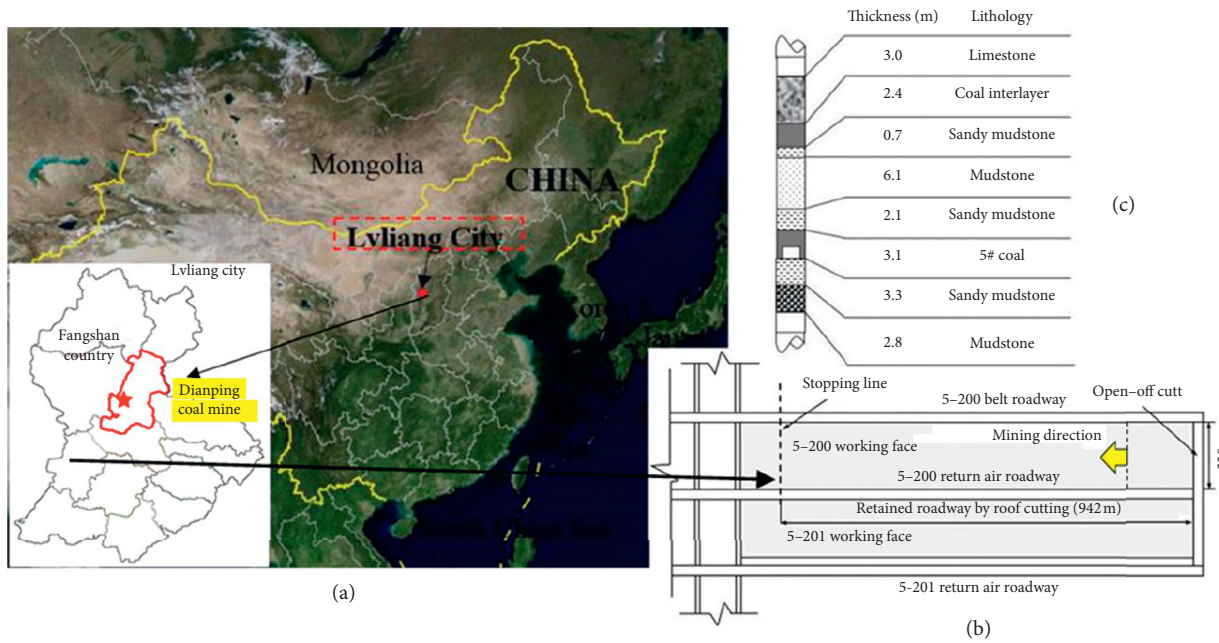

Figure 8: Engineering conditions.

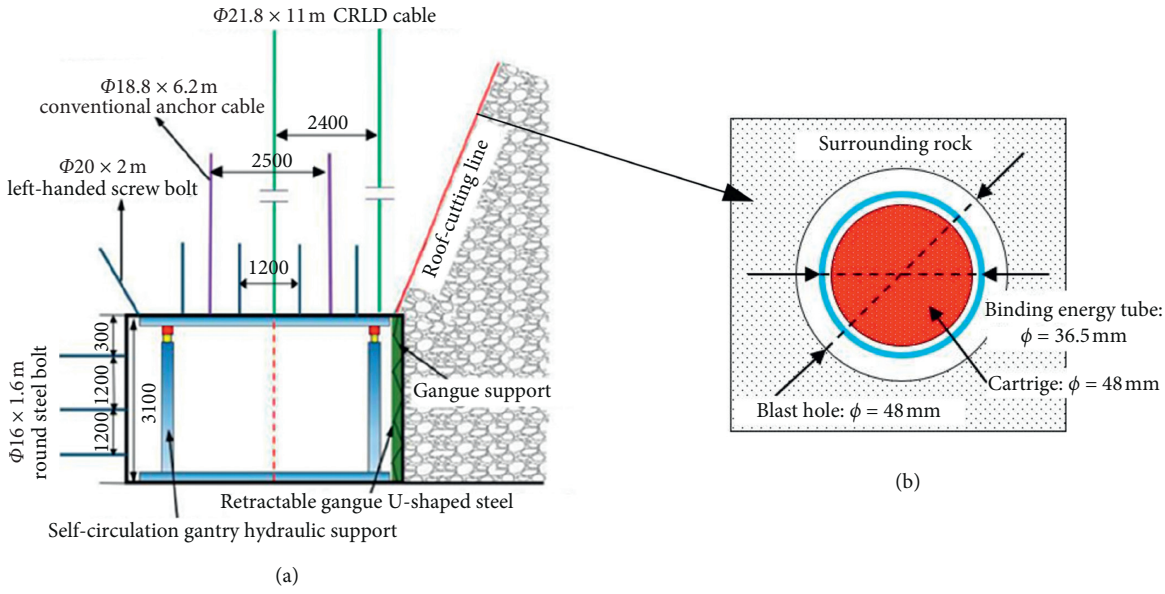

Figure 9: (a) Retained roadway support design. (b) Blasthole section.

between blasting holes was 500 mm. The binding energy tube is made from a special PVC material to control blasting energy. The device surface has two distributed rows of energy-accumulated grooves at 180° from each other with a spacing of 8 mm. The length of the binding energy tube is 1.5 m, the optimal sealing clay length was 2 m, the cartridge size was Φ27 × 300 mm, and the quality was 200 g/volume.

25# U-shaped steel shrinkable support is used to support the gangue after the support. The retractable 25# U-shaped steel is overlapped by upper and lower sections, the overlapping length is not less than 1 m, the steel shed length is 2.0 m and 2.5 m (it can be adjusted and matched according to the roadway height), two pairs of Kalan are used for connection, and the distance between the upper and lower edges of Kalan and the overlapping end of U-shaped steel is 50 mm respectively. 25# U-shaped steel shed shall be buried no less than 300 mm below the bottom plate.

4. Numerical Simulation

4.1. Model Establishment. To further study the evolution law of stress and displacement of roadway surrounding rock after roof cutting, the FLAC3 D numerical software was used to simulate three types of GSER, that is, the remaining coal pillar, wall building, and roof-cutting type based on the original size of the site [27–30]. As shown in Figure 10(a), a

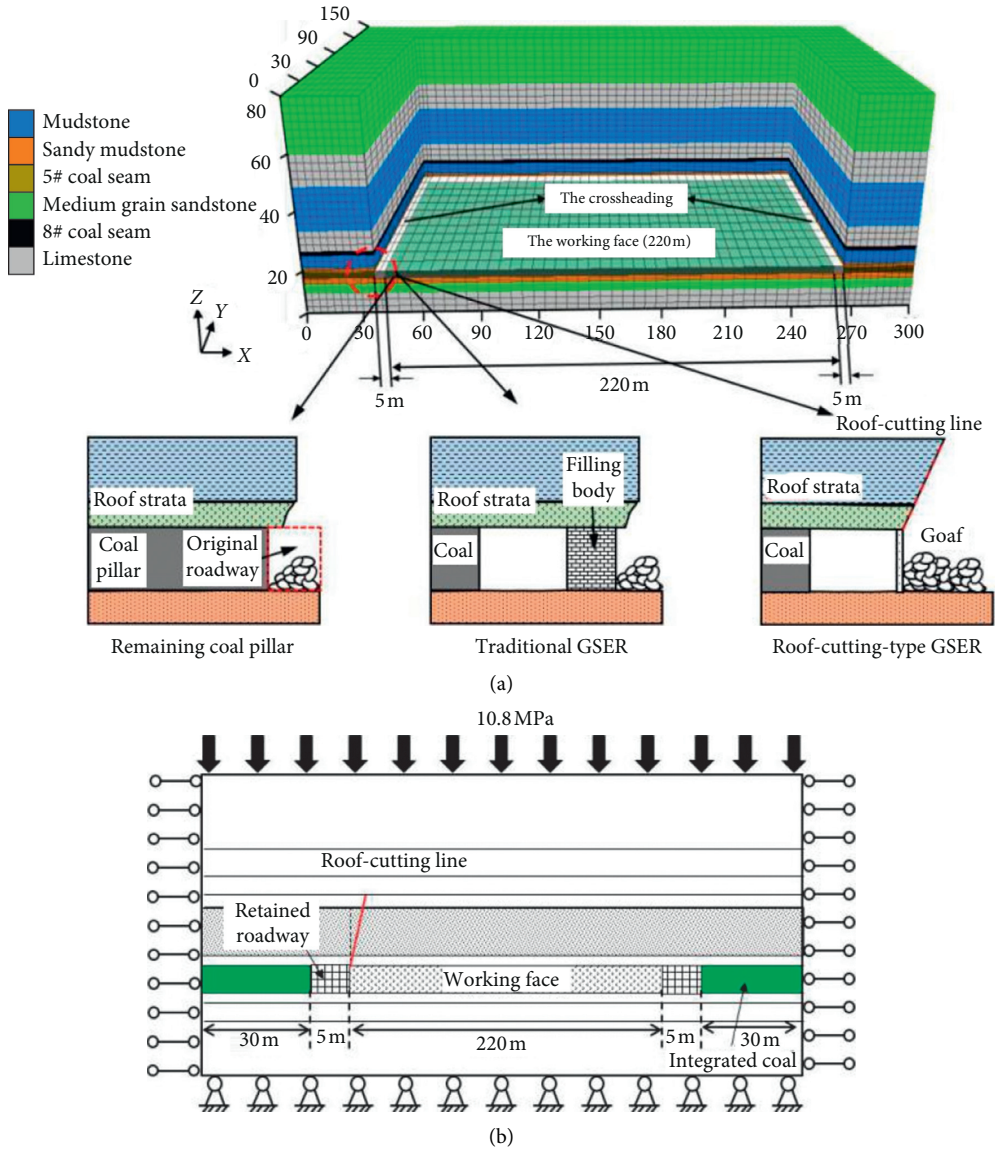

Figure 10: Numerical model.

numerical calculation model was established. The model dimensions were as follows: $x \times y \times z = 300 \times 150 \times 80$ m, the excavation size of the simulated roadway was $x \times y \times z = 5 \times 150 \times 3$ m, and the working face excavation size was $x \times y \times z = 220 \times 120 \times 3$ m. The numerical models under the three processes were basically the same, except for the marked dotted line in the figure, which was different at the reserved roadway. The first type is coal pillar mining, the second type is traditional GSER, and the third type is roof-cutting-type GSER. Figure 10(b) shows the model boundary conditions. The left and right boundaries of the model limit the displacement in the x-direction. The anterior and posterior boundaries limit the displacement in the y-direction and set the horizontal stress gradient, the lower boundary limits the displacement in the z-direction, and the upper boundary imposes uniform self-weight stress. The model failure complies with the Mohr–Coulomb strength criterion.

Table 1 shows the physical and mechanical parameters of each rock layer in the numerical model. As the roof and floor rock layers are mainly dominated by mudstone and sandy mudstone, the relevant indoor rock mechanics tests have also been performed in the second section. Thus, the experimental data can be directly applied. The other mechanical parameters such as medium grain sandstone and limestone are provided by the mine side.

5. Stress Distribution Law under Different Mining Technologies

5.1. Surrounding Rock Stress. Figures 11(a)–11(c) show the stress distribution of the roadway surrounding rock under the conditions of three retaining roadway technologies, and Figure 11(d) shows the solid coal side stress curve. The distance between the stress concentration area and the coal wall is relatively close under the three types of roadway

Table 1: Main physical and mechanical parameters of the model.

Rock strata	Bulk modulus/ 10^9 Pa	Shear modulus/ 10^9 Pa	Friction(°)	Compressive strength/ 10^6 Pa	Density/10^3 kg/ m^3	Cohesion/ 10^6 Pa
Limestone	16	17	36	5.9	2.5	5.6
Sandy mudstone	9	9	30	3.7	2.1	1.5
Mudstone	11	12	33	4.9	2.4	3.5
5# coal seam	1	2	30	0.6	1.4	1.1
Medium sandstone	13	15	38	4.9	2.4	5.4

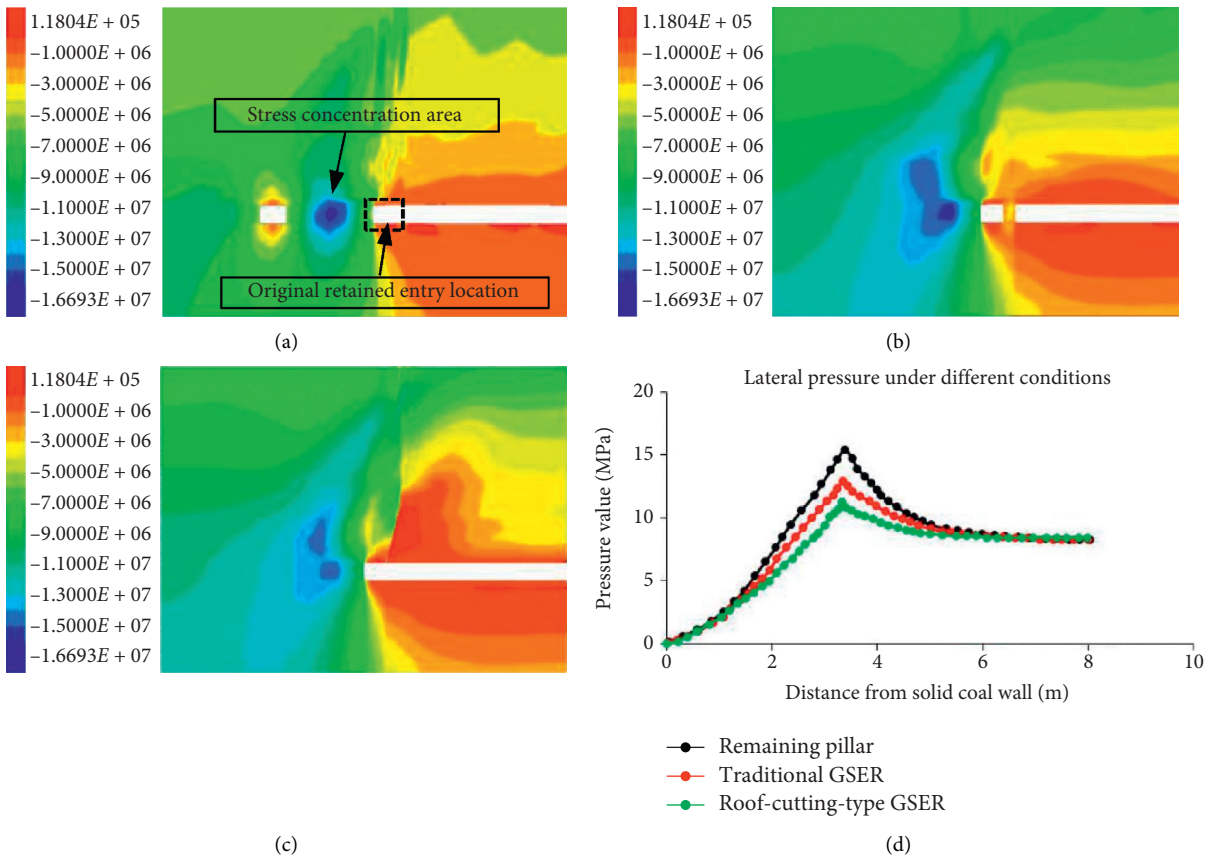

Figure 11: Surrounding rock stress under different mining conditions.

retention processes, and the side abutment pressures are 15.9, 14.1, and 12.1 MPa under the conditions of retaining coal pillars, retaining roadways with the traditional filling body, and roof cutting, respectively. In addition, compared with the traditional stress nephogram, the low-stress area of the roof is larger, which indirectly indicates that the roof cutting improves the stress distribution of the surrounding rock.

5.2. Stope Stress. Figure 12(b) shows the stress nephogram and curve at the position of the 5 m monitoring line in front of the working face. The advanced stress distribution rule and stress value of the working face are close under the conditions of the remaining coal pillar and traditional roadway reservation. However, under the condition of roof cutting, the stress clearly decreases, and its transverse influence range is approximately 60 m; that is, the roof-cutting-type GSER improves the stress distribution and also reduces the advanced stress concentration to a certain extent, which is conducive to the safe operation of the working face.

5.3. Research on Roof Cutting

5.3.1. Different Roof-Cutting Heights. From the above analysis, the stress distribution of the surrounding rock under the condition of roof cutting has been optimized to a certain extent. To obtain the best optimization effect, different roof-cutting heights and angles were simulated and analyzed to obtain the best roof-cutting parameter. Figure 13 shows the distribution law of the retained roadway surrounding rock stress under different roof-cutting heights.

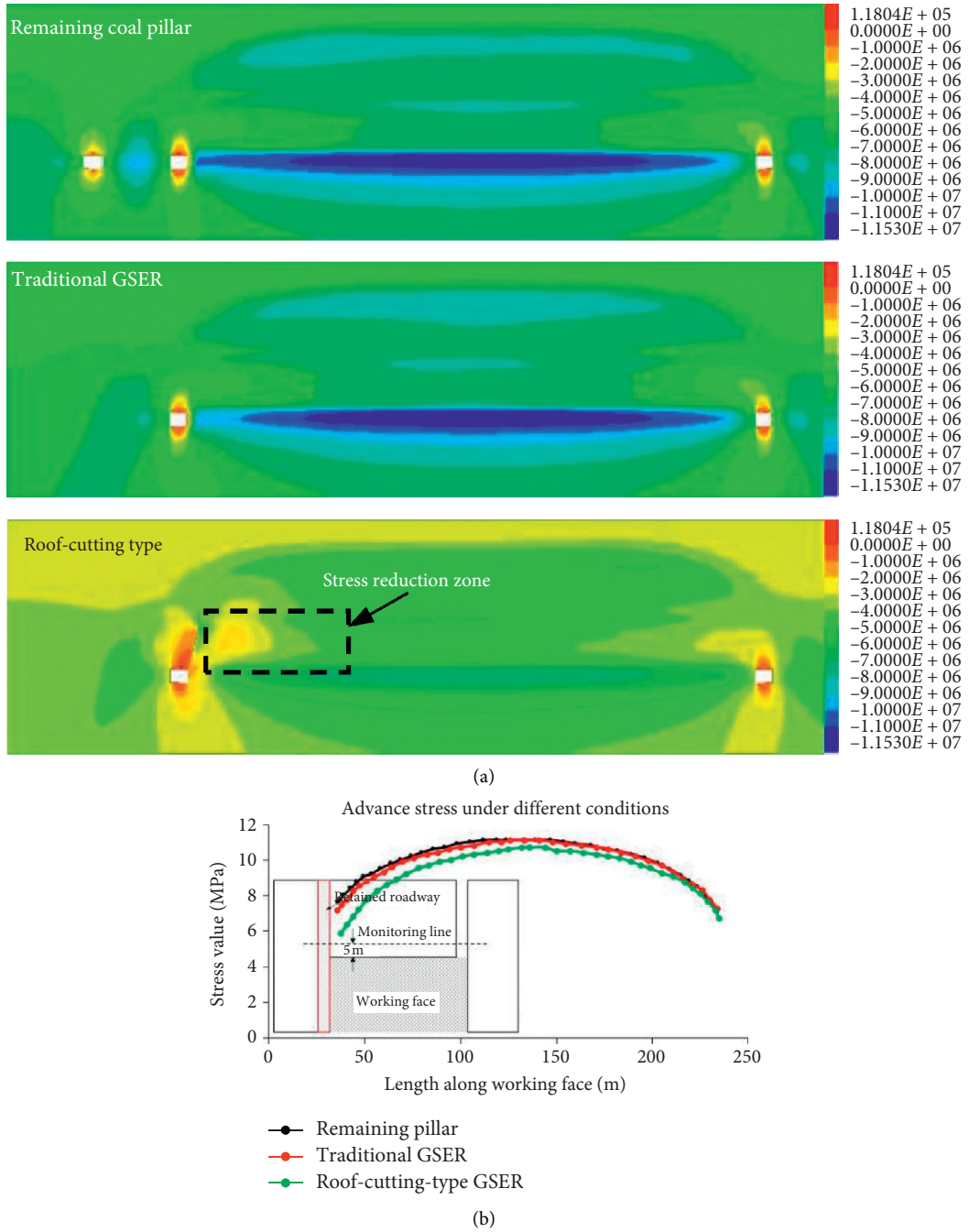

Figure 12: Stope advanced stress. (a) 5 m ahead of working face. (b) Stress curve.

When the roof-cutting height is 6, 8, and 10 m, the peak values of stress concentration are 13.0, 12.1, and 11.4 MPa, respectively. From 6 to 10 m, the stress decreases by approximately 11%, and the stress concentration area transfers to the deep position of the entity coal. From Figure 13(d), it can be seen that the larger the roof-cutting height, the smaller the peak stress, and the farther the stress concentration area is from the coal wall, the more beneficial it is to maintain the roadway. However, when the cutting height reaches a certain degree, it has little influence on stress reduction; therefore, the height of the roof cutting should be higher than or equal to 8 m but lower than 10 m.

5.3.2. Different Roof-Cutting Angles. Figure 14 shows the distribution law of the retained roadway surrounding the rock stress under different roof-cutting angles. It can be seen that when the roof-cutting angles are 0°, 15°, and 25°, the peak values of stress concentration are 12.1, 10.9, and 11.7 MPa, respectively. From Figure 13(d), when the angle is 0° and 25°, the stress value is relatively large but similar for 15°, and the peak value is the least. Thus, 15° provides the best results.

The above analysis indicates that the roof-cutting-type GBER can effectively interrupt the stress transfer path between the roadway and the gob roof strata, considerably

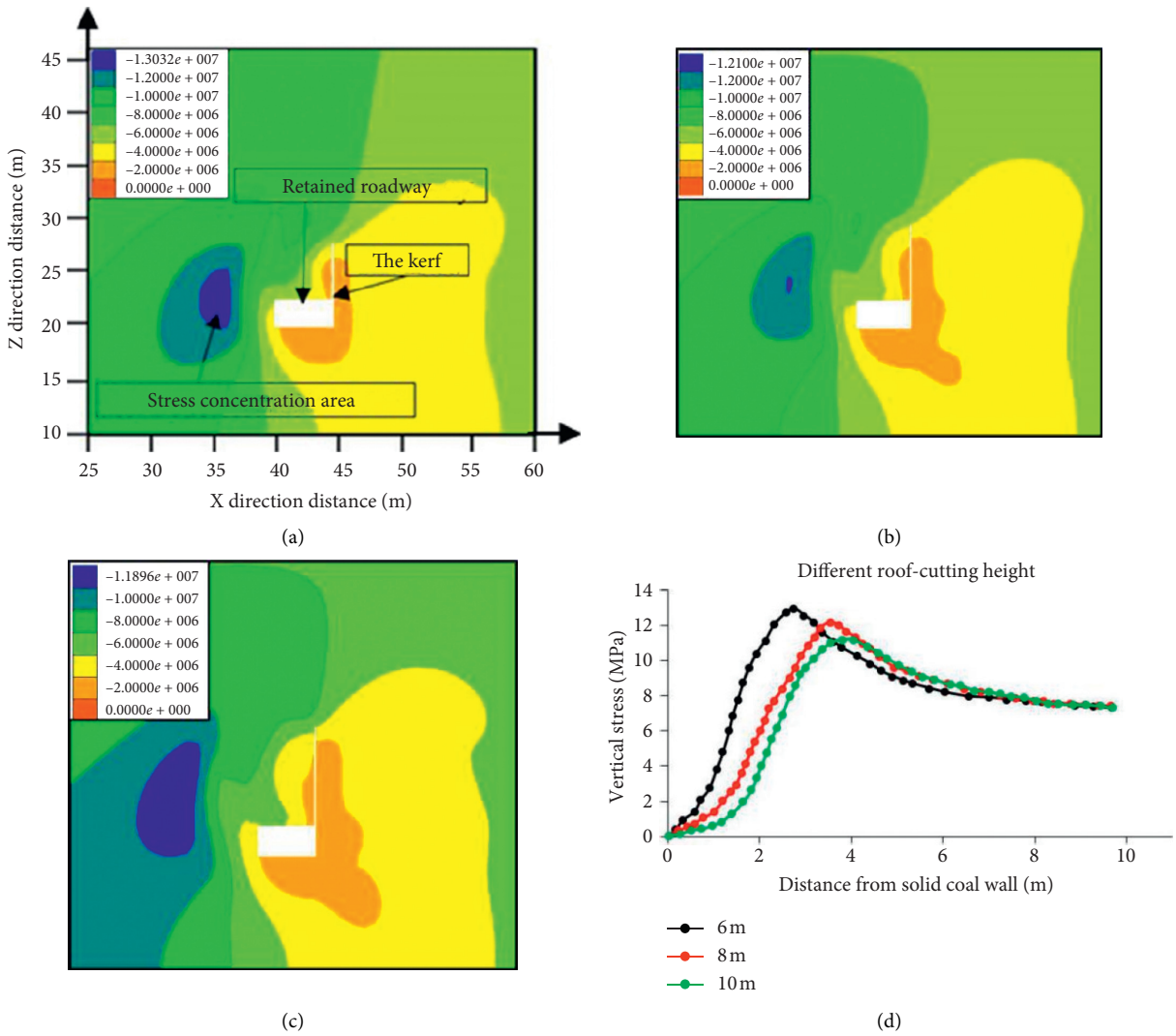

Figure 13: Vertical stress for the roof-cutting height of (a) 6, (b) 8, and (c) 10 m. (d) Surrounding rock stress curve.

reducing the peak value of stress concentration, distancing the concentration area from the coal wall, and transferring to the deep position of the entity coal. Owing to the roof cutting, the continuity of the roof over the roadway and the gob is interrupted; therefore, the roof deformation of the roadway is less affected by the movement of overlying strata over the gob.

5.4. In Situ Monitoring. After adopting the technology of GSER by roof cutting, it is necessary to monitor the deformation and stress of the roadway and working face to further formulate protective measures. The monitoring includes two aspects: the monitoring of the working face pressure and the appearance of the mine pressure monitoring in the retained roadway, including the stress of a single pillar and anchor cable, the pressure of retaining gangue, and the deformation of the roadway. Figure 15 shows the layout of the monitoring points. The working face hydraulic support is numbered from the cutting side to the rightmost side, starting from bracket 3#, and for every 10 brackets, a monitoring point is set up. Because the single prop is installed after mining, it lags behind the working face and sets a monitoring point every 20 m. The gangue retaining pressure monitoring points lag the working face and are arranged every 20 m. The layout of the CRLD cable stress monitoring points and roadway deformation monitoring points are the same. Starting from the position of the open-off cut, one monitoring point is set every 50 m.

5.5. Working Face Pressure Monitoring. Figure 16 shows the stress curves of the 5# hydraulic support. From the stress monitoring curve, when the roof cutting was performed, the stress value clearly decreased, the peak stress decreased from 56 MPa to 44 MPa, the average stress decreased from 43 MPa to 37.5 MPa, and its average periodic weighting length increased from 12 m to 21 m. The increase in the periodic weighting step indicates that under the influence of roof cutting, the overlying strata collapse height beside the cutting surface was large, the rock fragmentation was small, and the goaf filling effect was good. Therefore, there was less

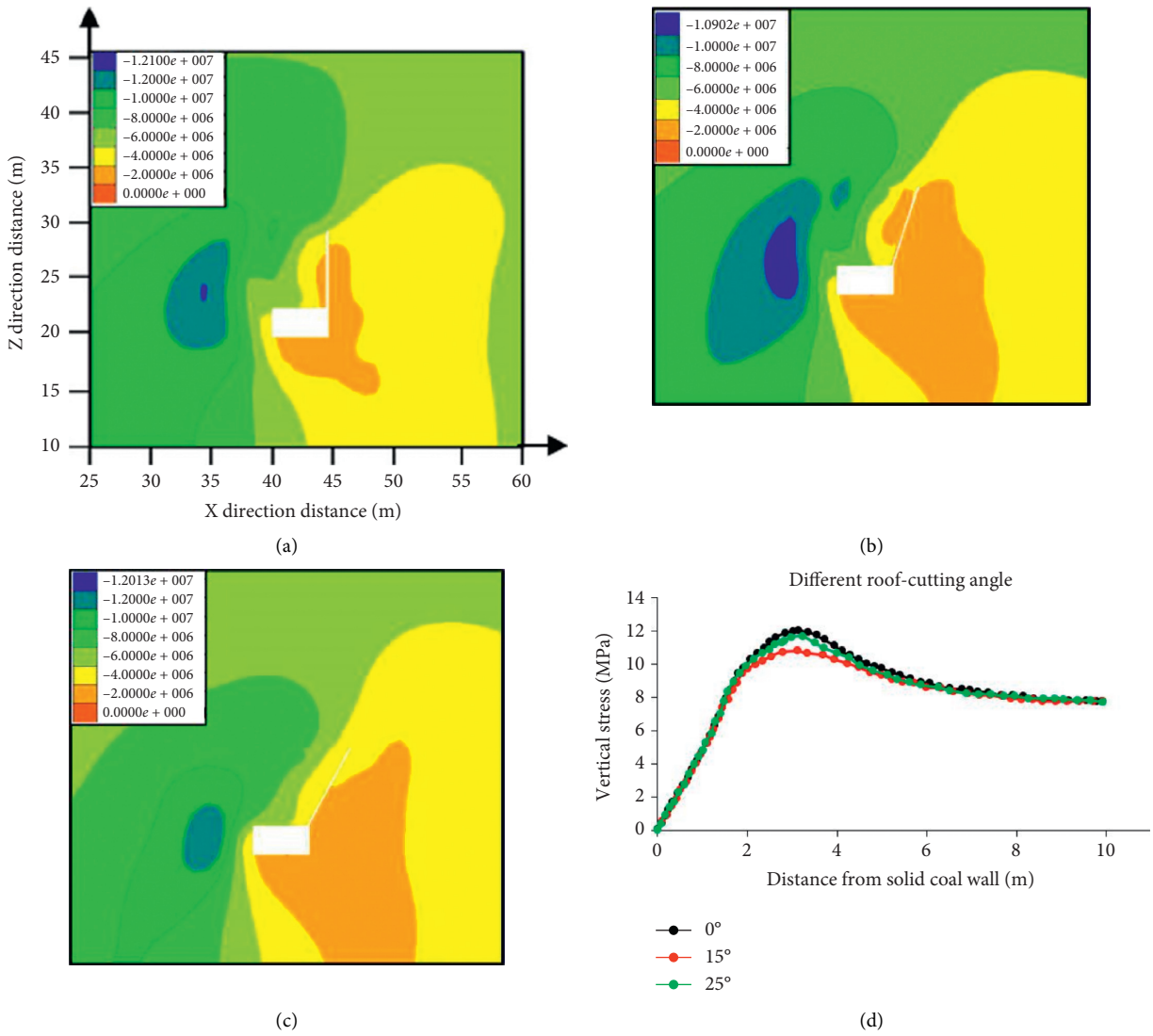

Figure 14: Vertical stress for roof-cutting angles of (a) 0°, (b) 15°, and (c) 25°. (d) Surrounding rock stress curve.

space for the main roof to rotate, the rotation angle was smaller, and the rotation deformation was also relatively small, resulting in the main roof difficult to fracture; that is, the fracture weighting step increased.

5.6. Mine Pressure Monitoring in Roadway

5.6.1. Stress Analysis of Single Hydraulic Prop and CRLD Cable. Figure 17 shows the stress curve of the CRLD anchor cable and single prop. The CRLD anchor cable measuring point is marked as M4 and is 230 m away from the open-off cut. The single prop measuring points are 690, 710, 730, 750, and 770 m away from the open-off cut. The cable curve can be divided into four stages: advanced impact, intense impact (the support resistance sharply increases), steadily increasing resistance, and stabilization stages. The intense impact zone is within 30 m before and after the working face, and the lead abutment pressure and roof movement caused by mining at this stage have the highest impact. When the measuring point lags the working face by approximately 100 m, the anchor cable enters the constant resistance stage. The stress variation of a single prop is consistent with that of the CRLD anchor cable. Within the range of 20 m behind the working face, the prop pressure sharply increases. After lagging the working face at 25 m, the prop pressure basically reaches a stable state, which indicates that the strata movement is initially stable.

5.6.2. Stress Analysis of Retaining Gangue. The caved gangue is used as part of the retained roadway, and the study of the gangue pressure on the lateral support system and the gangue collapse degree have important significance for the stability. Therefore, it is necessary to conduct dynamic monitoring and research on the gangue pressure on the lateral support and the coefficient of bulk increase in the field. Figure 18 shows the stress of retaining gangue and the coefficient of the bulk increase curve. When the measuring point lags behind the working face by approximately 100 m,

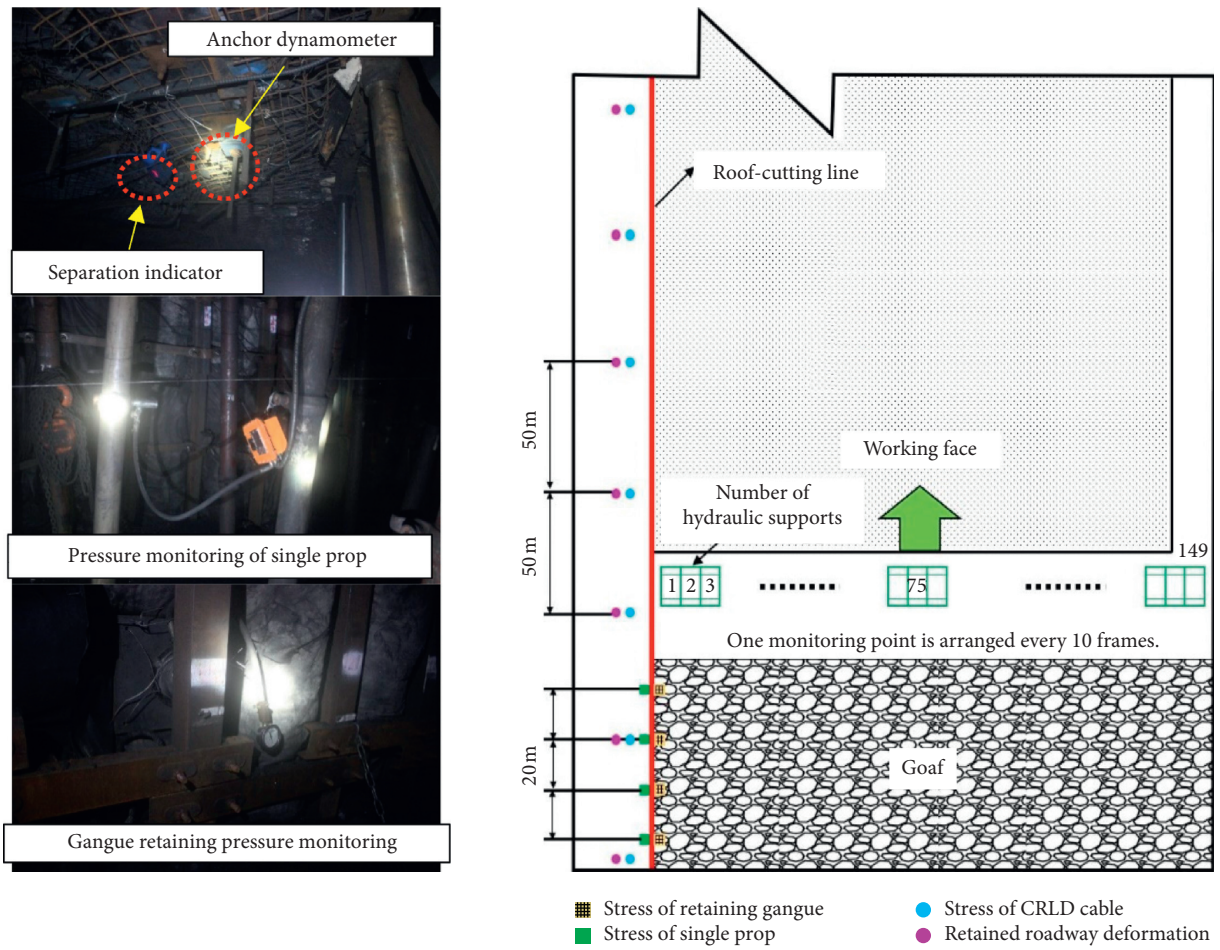

Figure 15: Layout of monitoring points.

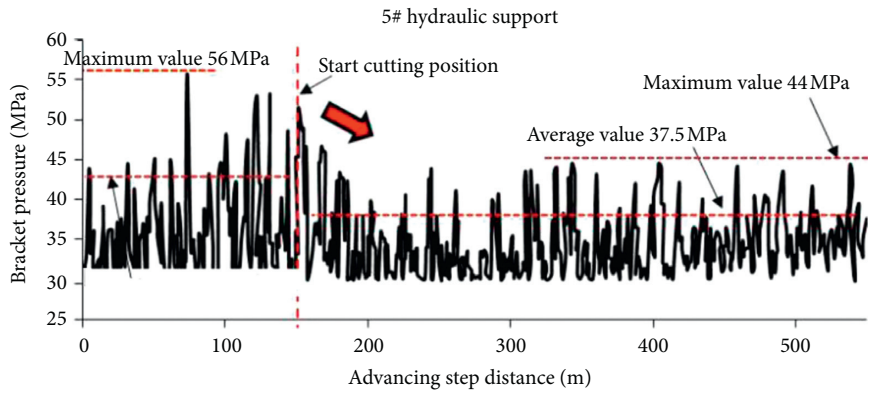

Figure 16: Stress curves of hydraulic support.

the gangue retaining pressure and coefficient gradually reach a stable state and exhibit a certain synergy. The maximum pressure is 2.9 MPa, and the average value is 1.93 MPa; the final coefficient of bulk increase is approximately 1.32.

5.6.3. Deformation Analysis of Retained Roadway. Figure 19 shows the displacement curve of the 8# measuring point. The measuring point is 160 m distant from the open-off cut. From the monitoring curve, it can be seen that the amount of roof subsidence is approximately 200 mm, the amount of floor heave is approximately 313 mm, and the convergence between roof and floor is 513 mm. When a single pillar is withdrawn, the deformation rate of the roadway increases, but the increase is small. When the measuring point lags behind the working face by approximately 300 m, the deformation of the roadway gradually stabilizes. Figure 20 shows the effect of the retained roadways in this coal mine.

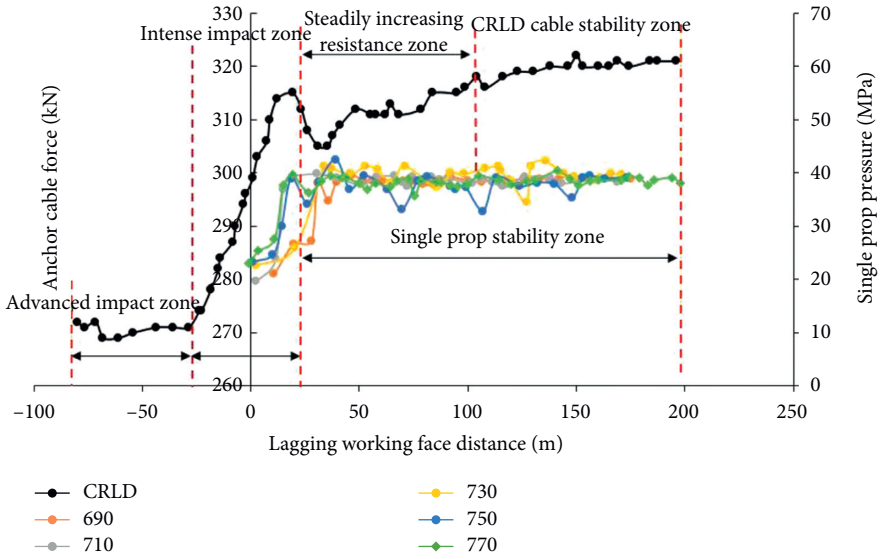

Figure 17: Force curve of CRLD anchor cable and single prop.

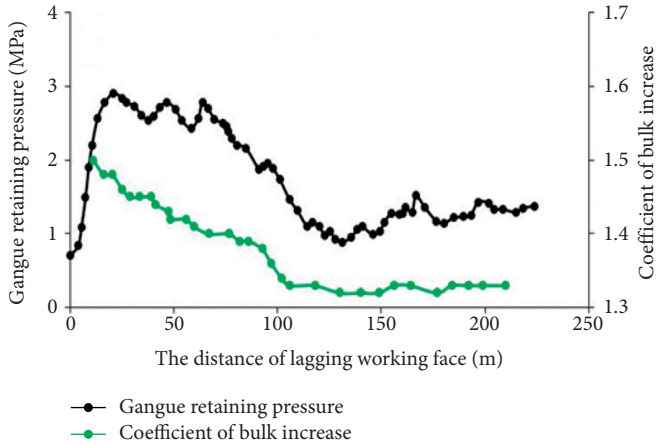

Figure 18: Change curve of stress and coefficient.

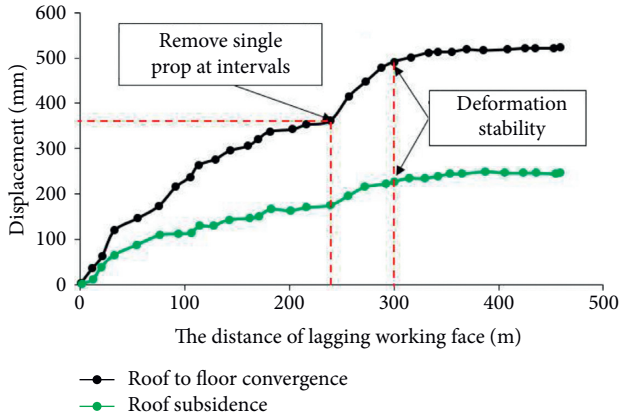

Figure 19: Displacement of roadway deformation.

(a) (b)

Figure 20: Effect of the retained roadway.

6. Conclusions

This study mainly analyzes the application of roof-cutting-type GSER in the medium-thick coal seam of the Dianping coal mine, in the Liliu mining area, and Shanxi province. First, the technological process and its technical principle were studied in detail, and mechanical analysis of the surrounding rock structure was performed. On this basis, the field parameter was designed, and the displacement and stress evolution law under the technical condition of the reserved roadway was studied using a numerical model. Finally, field monitoring was used to verify and evaluate the effect of the reserved roadway. The conclusions are as follows:

(1) The principle of roof-cutting-type GSER is to cut off the voussoir beam structures which were used to transmit horizontal thrust above the retained roadway due to the coal mining to achieve the purpose of optimizing the stress distribution of surrounding rock. The roof-cutting-type GSER has three core technologies: CRLD anchor cable strengthening support, roof cutting by directional blasting, and gangue retaining support, and through the study of these technologies, the basic technical parameters were determined; i.e., two rows of CRLD anchor cables were arranged; with the spacing of 1000 mm, the roof-cutting height and angle were designed as 9 m and 15°, respectively

(2) Based on the analysis of the surrounding rock structure formed by roof cutting, a mechanical model of the cantilever beam was established, and the calculation method of material mechanics was used to solve the support resistance and structural deformation. It is concluded that the closer to the roof-cutting side, the higher the displacement deformation

(3) Using FLAC3 D numerical simulation, the stress distribution laws under the three processes of retaining coal pillar, traditional wall building type GSER, and roof-cutting-type GSER were compared and analyzed. Under the condition of the remaining coal pillar and traditional GSER, the advanced stress distribution and value of the working face are close to each other, while under the condition of roof cutting, the advanced stress at the roof-cutting side decreases obviously, and its transverse influence range is about 60 m. On the basis of the above analysis, a simulation study was carried out on the roof-cutting-type GSER with different heights and angles, it was verified that the optimal cutting height was greater than 8 m and less than 10 m, and the optimal cutting angle was 15°. Above the analysis shows that roof cutting can effectively cut off the stress transfer between the roadway roof and the goaf, reduce the stress concentration degree, make the stress concentration area transfer to the solid coal, that is, to the side of roof cutting, and enhance the stability of the roadway roof

(4) On-site monitoring was performed, including the working face pressure, CRLD anchor cable, and single prop stress and roadway deformation. The field monitoring results showed that the preliminary weighting step of the roof-cutting side was larger than that of the uncut side, and the maximum mining face pressure was lower. The amount of roof subsidence was approximately 200 mm, the amount of floor heave was approximately 313 mm, and the overall deformation was small. This indicates that the effect of the retained roadway was good [31, 32]

Data Availability

The data used to support the findings of this study are available from the corresponding author upon request.

Conflicts of Interest

The authors declare that there are no conflicts of interest regarding the publication of this paper.

Acknowledgments

This research was funded by the National Natural Science Foundation of China, under grant no. 51574248, and the National Key Research and Development Program, under grant no. 2016YFC0600901.

References

[1] X. Z. Hua, "Development status and improvement suggestions for supporting technology of gob side entry retaining in China," *Coal Science and Technology*, vol. 12, pp. 78–81, 2006.

[2] A. Vakili and B. K. Hebblewhite, "A new cavability assessment criterion for longwall top coal caving," *International Journal of Rock Mechanics and Mining Sciences*, vol. 47, no. 8, pp. 1317–1329, 2010.

[3] R. Bertuzzi, K. Douglas, and G. Mostyn, "An Approach to model the strength of coal pillars," *International Journal of Rock Mechanics and Mining Sciences*, vol. 89, pp. 165–175, 2016.

[4] M. Alber, R. Fritschen, M. Bischoff, and T. Meier, "Rock mechanical investigations of seismic events in a deep longwall coal mine," *International Journal of Rock Mechanics and Mining Sciences*, vol. 46, no. 2, pp. 408–420, 2009.

[5] C. O. Karacan, "Prediction of porosity and permeability of caved zone in longwall gobs," *Transport in Porous Media*, vol. 82, no. 2, pp. 413–439, 2010.

[6] Q. M. Chen, "Characteristics of underground pressure and its control technology in fully-mechanized caving roadway," *Journal of China Coal Society*, vol. 8, pp. 382–385, 1998.

[7] H. P. Kang, D. L. Niu, Z. Zhang, J. Liu, and Z. Li, "Deformation characteristics and support technology of surrounding rock of deep gob," *Journal of Rock Mechanics and Engineering*, vol. 29, no. 10, pp. 1977–1987, 2010.

[8] Y. Tan, F. H. Yu, and J. G. Ning, "Design and construction of entry retaining wall along a gob side under hard roof stratum," *International Journal of Rock Mechanics and Mining Sciences*, vol. 77, pp. 115–121, 2015.

[9] H. Y. Yang, S. G. Cao, S. Wang, and X. Z. Chen, "Adaptation assessment of gob-side entry retaining based on geological factors," *Engineering Geology*, vol. 209, pp. 143–151, 2016.

[10] N. Zhang, L. Yuan, C. L. Han, J. H. Xue, and J. G. Kan, "Stability and deformation of surrounding rock in pillarless gob-side entry retaining," *Safety Science*, vol. 50, no. 4, pp. 593–599, 2012.

[11] L. S. Jiang, P. Wang, P. Q. Zheng, H. J. Luan, and C. Zhang, "Influence of different advancing directions on mining effect caused by a fault," *Advances in Civil Engineering*, vol. 2019, Article ID 7306850, 10 pages, 2019.

[12] Q. Wang, B. Jiang, R. Pan et al., "Failure mechanism of surrounding rock with high stress and confined concrete support system," *International Journal of Rock Mechanics and Mining Sciences*, vol. 102, pp. 89–100, 2018.

[13] G. S. P. Singh and U. K. Singh, "Prediction of caving behavior of strata and optimum rating of hydraulic powered support for longwall workings," *International Journal of Rock Mechanics and Mining Sciences*, vol. 47, no. 1, pp. 1–16, 2010.

[14] G. R. Feng, P. F. Wang, and Y. P. Chugh, "Stability of gate roads next to an irregular yield pillar: a case study," *Rock Mechanicas and Rock Engineering*, vol. 52, no. 8, pp. 2741–2760, 2019.

[15] Q. Wang, S. Gao, and B. Jiang, "Rock-cutting mechanics model and its application based on slip-line theory," *International Journal of Geomechanics*, vol. 18, no. 5, pp. 1–10, 2018.

[16] B. X. Huang, J. W. Liu, and Q. Zhang, "The reasonable breaking location of overhanging hard roof for directional hydraulic fracturing to control strong strata behaviors of gob-side entry," *International Journal of Rock Mechanics and Mining Sciences*, vol. 103, pp. 1–11, 2018.

[17] B. W. Wu, X. Y. Wang, J. B. Bai, X. X. Zhu, and G. D. Li, "Study on crack evolution mechanism of roadside backfill body in gob-side entry retaining based on UDEC trigon model," *Rock Mechanics and Rock Engineering*, vol. 52, no. 9, pp. 3385–3399, 2019.

[18] D. Fan, X. Liu, Y. Tan, Y. Lan, J. Ning, and S. Song, "An innovative approach for gob-side entry retaining in deep coal mines: a case study," *Energy Science Engineering*, vol. 7, no. 6, pp. 2321–2335, 2019.

[19] Q Wang, H. Gao, B. Jiang, S. Li, M. He, and Q. Qian, "In-situ test and bolt-grouting design evaluation method of underground engineering based on digital drilling," *International Journal of Rock Mechanics and Mining Sciences*, vol. 138, Article ID 104575, 2021.

[20] P. Wang, L. S. Jiang, J. Q. Jiang, P. Q. Zheng, and W. Li, "Strata behaviors and rock-burst-inducing mechanism under the coupling effect of a hard thick stratum and a normal fault," *International Journal of Geomechanics*, vol. 18, no. 2, pp. 1–14, 2018.

[21] Z. G. Tao, C. Zhu, M. C. He, and M. Karakus, "A physical modeling-based study on the control mechanisms of negative Poisson's ratio anchor cable on the stratified toppling deformation of anti-inclined slopes," *International Journal of Rock Mechanics and Mining Sciences*, vol. 138, Article ID 104632, 2021.

[22] Y. B. Gao, M. C. He, J. Yang, and X. G. Ma, "Experimental study on the roof cutting effect of empty coal gangue caving in automatic entry without coal pillar," *Journal of China University of Mining & Technology*, vol. 47, no. 1, pp. 21–31, 2018.

[23] E. Z. Zhen, Y. B. Gao, Y. J. Wang, and S. M. Wang, "Comparative study on two types of nonpillar mining techniques by roof cutting and by filling artificial materials," *Advances in Civil Engineering*, vol. 2019, Article ID 5267240, 15 pages, 2019.

[24] Q. Wang, M. C. He, J. Yang, H. K. Gao, B. Jiang, and H. C. Yu, "Study of a no-pillar mining technique with automatically formed gob-side entry retaining for longwall mining in coal mines," *International Journal of Rock Mechanics and Mining Sciences*, vol. 110, pp. 1–8, 2018.

[25] Y. B. Gao, Y. J. Wang, J. Yang, X. Y. Zhang, and M. C. He, "Meso- and macroeffects of roof split blasting on the stability of gateroad surroundings in an innovative nonpillar mining method," *Tunnelling and Underground Space Technology*, vol. 90, pp. 99–118, 2019.

[26] C. Zhu, M. C. He, M. Karakus, X. H. Zhang, and Z. G. Tao, "Numerical simulations of the failure process of anaclinal slope physical model and control mechanism of negative Poisson's ratio cable," *Bulletin of Engineering Geology and the Environment*, vol. 80, no. 6, pp. 3365–3380, 2021.

[27] M. C. He, W. L. Gong, J. Wang, Z. G. Tao, and Y. Y. Peng, "Development of a novel energy-absorbing bolt with extraordinarily large elongation and constant resistance," *International Journal of Rock Mechanics and Mining Sciences*, vol. 67, pp. 29–42, 2010.

[28] M. K. Abdul-Wahed, M. Al Heib, and G. Senfaute, "Mining-induced seismicity: seismic measurement using multiplet approach and numerical modelling," *International Journal of Coal Geology*, vol. 66, no. 1-2, pp. 137–147, 2006.

[29] Q. Wang, Z. H. Jiang, B. Jiang, H. K. Gao, Y. B. Huang, and P. Zhang, "Research on an automatic roadway formation method in deep mining areas by roof cutting with high-strength bolt-grouting," *International Journal of Rock Mechanics and Mining Sciences*, vol. 128, Article ID 104264, 2020.

[30] M. R. Islam, D. Hayashi, and A. B. M. Kamruzzaman, "Finite element modeling of stress distributions and problems for multi-slice longwall mining in Bangladesh, with special reference to the barapukuria coal mine," *International Journal of Coal Geology*, vol. 78, no. 2, pp. 91–109, 2009.